INTEGRATION OF SENTINEL-2 SATELLITE AND PROXIMAL SENSOR DATA FOR AGRICULTURAL MONITORING AND CROP HEALTH ANALYSIS

DR. LI WEI[1]*

[1]CHINESE ACADEMY OF SCIENCES, INSTITUTE OF REMOTE SENSING AND DIGITAL EARTH, BEIJING, CHINA

ABSTRACT

Considering the importance of crop production for the growing population of the world, timely and accurate information about crop development is essential for successful agricultural monitoring. With an increasing interest of the agricultural community in precision agriculture, there is also a growing interest for using different spectral vegetation indices derived by different sensor devices. They can offer a valuable perspective both at the field-scale and at the plant level. In order to better utilize the spectral reflectance measurements from different sensors for agricultural applications, as well as to promote synergistic use of proximal and remote sensing sensors in this area, this paper aims to compare two novel sensing approaches for crop monitoring; a) the recently developed active multispectral proximal sensor named Plant-O-Meter and b) Sentinel-2 satellite, which carries a multispectral optical instrument. Both sensors and sensing methods are suitable for agricultural applications, following the same basic measurement principles. In general, their operation is based on the estimation of the proportion of radiation that is reflected from the target, which in agricultural systems refers to plants or the soil, at different wavelengths of the spectrum of light. However, each of the two sensing systems shows pros and cons regarding the spatial, spectral and temporal resolutions, the need for corrections and calibrations and the dependency from external parameters such as the weather or illumination conditions. Therefore, their complementary use is expected to bring added value comparing to information retrieved by each sensor separately. In order to correctly address the problem of data fusion, compatibility studies between the two sensors (passive remote and active proximal) are necessary. In this study, a maize field was sensed on several dates in 2018 growing season using both the Plant-O-Meter active proximal sensor and images acquired by Sentinel-2. Numerous vegetation indices based on different spectral channel combinations were calculated and the results were compared using linear regression analysis. First results showed good positive correlations between the indices obtained by the two sensors which signify their joint potential, hence further development and research on this topic are appreciated and expected.

Keywords*:* crop monitoring, proximal sensing, Sentinel-2, vegetation indices, correlation

1. INTRODUCTION

Precision agriculture (PA) is often defined as a farming approach in which decisions are made at a high resolution according to the actual needs of the plants at each location. Precision agriculture is commercially practiced since the early 1990's (Mulla, 2013) when the yield monitors with georeferencing capability became commercially available (Yang et al., 2013). There are several definitions of PA. Fountas et al. (2016) defined PA as "the management of spatial and temporal variability in the fields using Information and Communications Technologies (ICT)". Khosla (2008) referred to the five "R's" of PA which correspond to the application of inputs in agricultural systems at the "Right time", at the "Right amount" and to the "Right place" (Robert, 1994), using "the Right Source", and the "Right manner"(Khosla, 2008).

In practice, in order to address all the aspects of PA, fields and plants are monitored using a variety of sensing technologies and decisions concerning fertilizer, pesticide, irrigation and field operations are

adjusted accordingly. PA management systems show significant advantages compared to traditional farming such as increased application efficiency, and minimal environmental footprint of agricultural applications (Auernhammer, 2001; Raun et al., 2002; Tagarakis et al., 2013; Tagarakis et al., 2017). However, recent advances in technology provide an unprecedented opportunity for further development. Remote and proximal sensing using optical sensors are gaining popularity in crop production systems in the framework of PA applications. Nowadays, there is vast number of optical sensors recording the data about crops at different spatial, radiometric and temporal resolutions. Both remote and in-field sensors are used for monitoring plant deficiency for nutrients and water, plant health status and soil condition (Lee et al., 2010). Regarding the platform carrying the sensor and the sensors' proximity from the target, they can be divided into three general categories, namely:

1. satellite-based sensors,
2. airborne and unmanned aerial vehicles (UAV)-mounted sensors,
3. ground-based proximal sensors.

Satellite-based sensors

The first and the uppermost level is remote sensing where information is derived from satellite images. In recent studies, satellite data are increasingly used to monitor agricultural fields since they present a powerful tool for monitoring phenological trends and assessing the effect of climate variability. Compared to hand-held optical sensors, satellite images offer a valuable perspective at the field-scale, revealing regional crop conditions that are difficult to detect from ground manual measurements due to limited sampling capabilities (Wang et al., 2016). This is by far the most scalable sensing technology, as satellites such as Sentinels by the European Space Agency (ESA), Landsats by the National Aeronautics and Space Administration (NASA) and many other commercial satellites, are covering the whole planet at different revisit frequencies providing images at spatial resolutions that may range from few decimeters to hundreds of meters (depending on the satellite and the sensor). Besides the visible range of the electromagnetic spectrum, many satellite sensors also employ red edge, near-infrared, infrared, and thermal domains, making them particularly valuable for crop monitoring (Tucker, 1979). Atzberger (2013) pointed out that satellite remote sensing shows great potential for monitoring vegetation dynamics due to large spatial coverage and frequent revisit time. Satellite remote sensing has been used in agriculture since the 1970's when the first Landsat satellite was launched. Over the period of nearly half a century, the resolution of satellite images, as well as the revisit frequency, increased dramatically (Mulla, 2013). Today, a variety of different satellites are used for agricultural monitoring purposes, including Planet satellites with a resolution of up to 3 m, RapidEye with 5 m resolution and Pleiades with 50 cm resolution, each having a daily revisit time. However, a big drawback of the aforementioned commercial satellites is that the images are not free of charge and the cost of monitoring are thus prohibitively high for the majority of the farms. In the last decade ESA and NASA changed their policies and made certain satellite imagery available to the general public at no cost (Woodcock et al., 2008; Aschbacher and Milagro-Pérez, 2012). Landsat's 40-year long archive is now freely available and the same holds for the state-of-the-art Earth observation program Copernicus operated by ESA on behalf of the European Commission. These led to an increased interest of the agricultural community towards satellite remote sensing in the previous years. Still, a few meter resolution of freely available satellite imagery may not be sufficient for precise monitoring of individual plants and could make the detection of fine differences within the field difficult. Another drawback of optical satellite sensors is the weather dependency. Clouds can heavily obscure images making them sometimes useless and that presents a serious challenge especially in rainy parts of Western Europe and North America. Satellites working in microwave domain like Sentinel-1 and TanDEM-X can, to a certain level, assist in this case since their signal penetrates clouds due to a different working principle. However, the

information collected is different compared to the optical sensors and this is still an area of active research (McNairn et al., 2009, Joshi et al., 2016).

Airborne- and drone-based sensors

At the second level, when higher resolution is needed, optical sensors carried by aircrafts or, more recently, unmanned aerial vehicles (UAVs) can be used. They can provide precise measurements at high spatial resolution (a few cm) and are an ideal tool for crops that need detailed images for monitoring such as orchards and vineyards, or any crops that don't fully cover the ground surface at the critical stage of image acquisition. The high cost of lifting an aircraft, the costs of equipment and operation, or the limited flight time of UAVs due to battery power limitations, are just some of the challenges in this category which make these solutions less scalable than satellite-based applications. However, there is an obvious and equally rising interest of the agricultural community in these techniques, with the UAV and the UAV-mounted sensors industry showing rapid growth.

Ground-based proximal sensors

Ground-based proximal sensing is performed by sensors at a relatively short distance from the object of interest. Hand-held devices or sensors mounted on tractors and other vehicles are usually referred to as proximal sensors, here referred as ground-based proximal sensors. Their limitation is the small area coverage (Jackson, 1986), but they also have significant advantages, such as high spatial resolution and independent choice of the time of acquisition. The typical spatial resolution of proximal sensing is in the range from millimeters to centimeters, as opposed to remote sensing that typically has resolution in the range from decimeters to hundreds of meters (Oerke et al., 2014). Another advantage is that their measurements are not compromised by cloudiness, in case of active sensors, and are ideal for practical applications such as on-the-go variable rate fertilization (Shanahan et al., 2008). Active proximal sensors are independent of illumination conditions, since they emit their own light, and can operate under cloudy conditions or even at night. Furthermore, they do not require calibration to reflectance because the light source is known and constant (Fitzgerald, 2010). However, the same is not applicable for passive sensors. Differences in environmental conditions between the start and end of measurement (Tattaris et al., 2016) occur due to time consuming character of ground-based sensing and this can reflect on losing precision in these types of measurements. Over the years, various different optical proximal sensors found practical applications, such as SPAD meter (Konica Minolta Inc., Osaka, Japan), Hydro N-sensor (Yara International ASA, Oslo, Norway), GreenSeeker (Tribmle Inc., CA, USA), Crop Circle (Holland Scientific, NE, USA), CropScan (Next Instruments, Sydney, Australia), ASD FieldSpec (ASD Inc., CO, USA), etc. Although they are least scalable, proximal sensors provide accurate assessment of the plants' growth, which is linked to photosynthetic activity and chlorophyll content (Adamsen et al., 1999), level of evapotranspiration (Helman et al., 2019), crops' nitrogen status (Stone et al., 1996; Raun et al., 2002; Tagarakis and Ketterings, 2018), and yield (Tagarakis and Ketterings, 2017; Tagarakis et al., 2017).

Vegetation indices

The development of low-cost sensors, as well as the aforementioned liberalization of data access by data providers such as the ESA and NASA, have paved the way for the acquisition of vast amounts of sensor data. Compatibility studies between datasets acquired by different sensors are necessary prior to any kind of data fusion in practice. These studies are usually relying on the calculation of vegetation indices (VIs) that are the base for analyzing growth and vigor of vegetation. Vegetation index is a combination of different spectral bands in which information about reflected electromagnetic radiance from vegetation canopy is stored.

Satellite and hand-held sensors are usually multispectral sensing devices operating in the visible (red, green and blue) and infrared wavelengths, which are especially interesting for agricultural monitoring. Due to variable lighting conditions or scanning angles among two or more measurement dates, absolute values of single band measurements are seldom used. On the other hand, relative difference between different bands is more stable as the additive effect of illumination on the response may be approximated as equal throughout the spectrum. For this reason, vegetation indices (VIs) have been developed in order to relate the reflected electromagnetic radiance from the canopy with the canopies' characteristics (Hatfield et al., 2008). VIs are more widely used than absolute reflectance values in remote sensing algorithms for monitoring crop characteristics because of their simplicity and the ease of data processing (Wang et al., 2016). Light of different parts of the electromagnetic (EM) spectrum acts differently when in contact with vegetation. In this regard, e.g., infrared light is reflected by mesophyll tissue whereas red light is absorbed by chlorophyll. Hence, their ratio will give high values for actively growing vegetation in contrast to stressed vegetation or other types of surfaces (Campbell and Wynne, 2011). Due to the increase in biomass, changes of near-infrared radiation reflected from the canopy are the greatest during the growing season, whereas visible light shows lower variation mostly related to absorption of light by photosynthetic and photoprotective pigments (Hatfield et al., 2008). Usage of VIs is very dependable on instruments and platforms that are recording this data (Xue and Su, 2017).

Various VIs have been used for assessing different phenomena, such as plants' vegetation characteristics (NDVI, Rouse et al., 1973), available soil moisture (NDWI, Gao, 1996), drought intensity (NMDI, Wang and Qu, 2007) etc. Today, NDVI is most widely used, but it has its limitations with most important the fact that it reaches saturation when the canopy is dense, usually at the end of the growing season (Huete et al., 2002). Generally, there is no perfect VI that could be used for all phenomena, all crops and all regions, and because of that, a variety of indices are used in scientific applications. The VIs can be affected by the canopy structure, leaf angles and their spatial distribution, plant row orientation, atmospheric conditions, which all together strongly influence canopy reflectance. They are generally mathematical expressions of the reflectance using just a few specific spectral bands and at a single-angle of observation (usually nadir sensor orientation), which leads to an under-exploitation of the full spectral and directional ranges available when using new generation sensors (Pasqualotto et al., 2019).

This might, however, change in the future by utilizing other techniques that are rising in trend nowadays. As it is usually the case with data-driven decision-support systems and monitoring applications, the more data are collected, the better. Nowadays, new approaches for data analysis are gaining popularity, providing the ability to analyze massive amounts of data and information. The essence of Big Data Analytics and Machine Learning is to acquire a huge quantity of data and leave it to the algorithm to find the hidden dependencies between them. Literature that convers machine learning for agriculture was recently reviewed by (Liakos et al., 2018) who reported that over 60% of the studies were related to crop management. Hence, a likely pathway in Agriculture 4.0 is, among other, the utilization of VIs and Artificial Intelligence.

Inter-comparison

Although proximal and remote sensing were extensively studied for assessing crop dynamics (Corti et al., 2018), direct inter-comparison between satellite remote sensing and proximal sensors with respect to the crop monitoring has rarely been discussed. Bausch and Khosla (2010) compared QuickBird satellite-derived indices with ground-based Exotech radiometer-derived indices and found good correlation, with the highest agreement in green normalized difference vegetation index normalized for reference area (NGNDVI). Caturegli et al. (2015) tested ground-based multispectral measurements (using Licor spectroradiometer and GreenSeeker) and GeoEye-1 satellite images for estimating nitrogen status of turfgrasses. Comparing NDVI values acquired from these instruments, the highest Pearson correlation coefficient was found between GreenSeeker and satellite derived NDVI ($r \approx 1$). Yang et al. (2008) found moderate linear correlation ($r > 0.7$) between NDVI measured from Formosat-2 satellite images and ground portable spectroradiometer GER-2600. Wagner and

Hank (2013) revealed Pearson correlation coefficient of 0.85 between RapidEye and YARA-N sensor-derived Red Edge Inflection Point (REIP). Necessary modification was made in RapidEye measurements using YARA-N sensor-based model, so that the REIP could be calculated. Bu et al. (2017) confirmed that yields of sugar beetroot, spring wheat, corn and sunflower can be predicted with GreenSeeker, Crop Circle and RapidEye red and red-edge imagery.

The use of VIs is of great importance in monitoring crop dynamics and predicting end-of-season yield from mid-season canopy reflectance measurements. Hence, it is essential to quantify the level of similarity between different sensor measurements prior to data fusion. Jackson and Huete (1991) pointed that caution is needed when comparing VIs obtained by different sensors because of the differences between sensors' band-response functions, the differences in the fields of view, and the type of data, raw or transformed, acquired by each sensor.

In this chapter, 17 different indices were analyzed and their importance for crop monitoring, their stability and applicability on a large scale were discussed. VIs were derived from measurements made with a recently developed, active, multispectral proximal sensor named Plant-O-Meter (POM) and compared to VIs derived from Sentinel-2. The first practical value of this research lies in the fact that POM measurements could serve as the ground-truth for calibration of satellite images in large-scale applications. In this way, data with coarser spatial resolution and lower accuracy could be fine-tuned to fit the field measurements and provide higher accuracy results for broader areas swept by the satellite. Additionally, the motivation behind this research was to correlate measurements from a novel device with measurements widely used in modern research purposes. Nevertheless, both sensors represent modern optical instruments that are likely to find broader use in the near future.

2. MATERIALS AND METHODS

The present study was carried out during the 2018 growing season at a commercial field located in Begeč (45°14' 32.712" N and 19° 36' 21.486" E), near Novi Sad, in Vojvodina (Serbian province). The study area covers a geographical area of 6 ha. The experimental field's soil properties were favorable for maize production showing high content of humus and nutrients, and neutral to slightly alkaline reaction, typical characteristics of the chernozem soils which are dominant in the area. The climate of Vojvodina is moderate continental, with cold winters and hot and humid summers with huge range of extreme temperatures and nonequal distribution of rainfall per month (Hrnjak et al., 2014). The mean annual air temperature is 11.1 °C and the cumulative annual precipitation is about 606 mm according to climate data from the period 1949–2006 (Gavrilov et al., 2010). During vegetation periods of maize (from April 1 to September 30), the total cumulative precipitation was about 398 mm, which was 10% more than the 1970-2018 period average (Figure 1, Radičević et al., 2018).

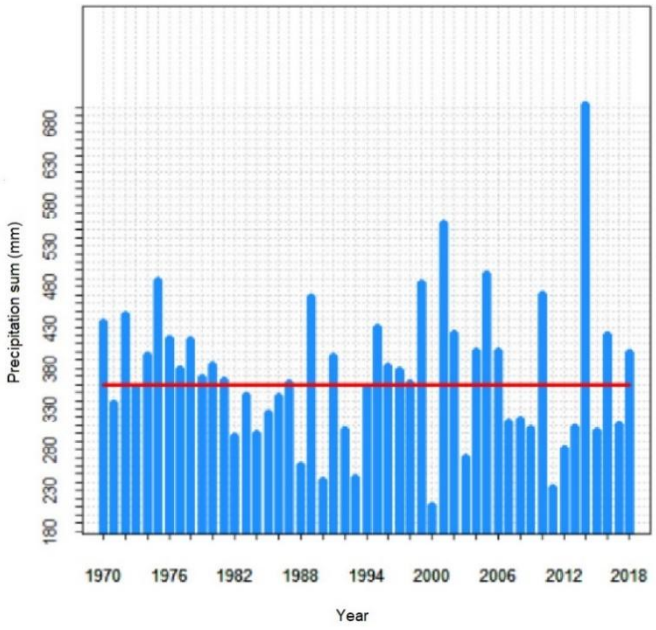

Figure 1. Precipitation sum (mm) in Serbia for 1 April – 30 September 2018. In vegetation period 2018 it was recorded about 398 mm of precipitation, i.e. cca 10% above the average (Radičević et al., 2018).

During maize planting season, extremely dry and warm weather was recorded. Increased daily air temperatures in late April and early May accelerated maize development stages. However, the period from June to August was more humid and warmer compared to the average climatic conditions for the region. The soil conditions regarding soil moisture content were monitored using a wireless network of soil moisture sensors; 3 sensor nodes installed in specific locations according to soil apparent electrical conductivity zones. The crop was irrigated after seeding to enhance germination and support growth during the initial growth stages. Two additional irrigations were supplied in critical stages when the water demand is high; in June after V6 growth stage when rapid growth occurs and in August during grain filling stages. On the other hand, September was significantly dry, which was particularly favorable for maize crop allowing for the grain to mature and dry. The meteorological data, (air temperature and precipitation) were acquired from the official web portal of the Hydro-meteorological Service of the Republic of Serbia (www.hidmet.gov.rs). The field was sown with "Exxupery" (by RAGT Semences, France, FAO 560) maize hybrid (*Zea mays* L.) widely adopted by farmers in Europe. Maize field was sown on April 15, 2018 for the major cropping season. Seeding was done in 300 m long rows, at the plant distance of 0.2 m within rows and 0.7 m between rows. Maize was grown using common agronomic practices to avoid any nutrient deficiencies and other unfavorable conditions. A total of 300 kg ha^{-1} of composite granular synthetic fertilizer (15:15:15; N-P-K) was applied at planting. The field was harvested when the majority of plants reached full maturity, on September 30, 2018.

Plant-O-Meter

In-field proximal measurements were performed using POM sensor, an active crop sensor, recently developed by BioSense Institute (Republic of Serbia). It is a multispectral sensing device emitting at four wavelengths of the electromagnetic spectrum: blue - 465 nm, green - 535 nm, red - 630 nm and near-infrared - 850 nm and measuring the amount of energy reflected by the target. Based on these measurements, a number of vegetation indices can be calculated. As previously explained, these indices represent combinations of surface reflectance at two or more wavelengths and they have been adopted with the aim to highlight particular properties of the scanned plants (Bannari et al., 1995). The multispectral source is developed using four super bright LED dices that emit radiation at

the defined wavelengths and have been attached on a surface mounted technology (SMT) chip, Figure 2.

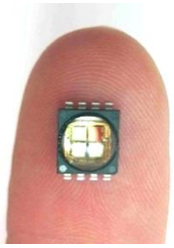

Figure 2. SMT multispectral source with four wavelengths: 850, 630, 535 and 465 nm.

The reflected light is detected by a silicon PIN photodiode BPX 61 (OSRAM Opto Semiconductors, 2015) with supporting electronics for filtering and amplifying the useful signal as well as for providing immunity to ambient light up to 10,000 lux. This photodiode-based detector module sequentially receives the reflected spectrum and sends the raw data to the microcontroller which averages the measurements and sends the data via Bluetooth to Android-operated device such as tablet, smartphone or similar. All further processing is performed using the processor of the Android device through a specially designed Android application. Each measurement is georeferenced using the internal antenna of the Android device (which typically support GPS, GLONASS, or Beidou systems). Based on these inputs, VIs are calculated and displayed on the screen through the POM Android interface. The application has two operating modes 1) stationary measurements used for recording unique georeferenced measurements of specific locations in the field, and 2) continuous measurement intended for mapping the plants' canopy or soil reflectance in the field. More detailed information about POM sensor (Figure 3) and its operating principles can be found in the dedicated paper (Kitić et al., 2019).

Figure 3. Plant-O-Meter and specially developed Android application.

During the field ground-based proximal measurements, the POM was used to scan the whole length of every tenth row by walking along the rows, holding the sensor directly on top of the crop row with the scanning footprint perpendicular to the row direction. The measuring frequency was 1 Hz, which roughly corresponded to 1 m distance between the POM record points along the row. POM measurements were performed at four different dates and were carried out in the following stages of maize development: 6-leaf growth stage (V6), beginning of tasseling (VT), silking (R1) and at the end of blister stage (R2), (Table 1).

Table 1. Corresponding acquisition dates for POM and Sentinel-2 and development stage of maize.

POM date	Sentinel-2 date	Crop development stage
01.06.2018	30.05.2018	6-leaf (V6)
21.06.2018	24.06.2018 (cloudy)	Tassel (VT)
04.07.2018	14.07.2018	Silking (R1)
26.07.2018	29.07.2018	Blister (R2)

Table 2. Operating wavelengths for POM and Sentinel-2.

	Plant-O-Meter	Sentinel-2 [nm]		
Band name	**Wavelengths range [nm]**	**Central wavelength [nm]**		**Bandwidth [nm]**
Blue	450-465	490		65
Green	520-535	560		35
Red	620-630	665		30
NIR	830-870	**Wide**	842	115
		Narrow	865	20

Sentinel-2

Sentinels are series of space missions of the European Union's Copernicus programme which was created for monitoring the Earth's environment (Aschbacher, 2017). Each mission is specifically designed and is using different technology to collect various type of information about Earth's land, water, and atmosphere. Sentinels -1, -2, -3 and -5P have currently been launched. Sentinel-2 is a constellation of two identical satellites A and B, launched respectively on June 23, 2015 and March 7, 2017. They fly at the average altitude of 786 km, in the same orbit phased at 180° to each other (Pandžić et al., 2016), thus having joint revisit time of 5 days at the equator. Sentinel-2's swath width is 290 km and it images the Earth's surface between 56° S and 84° N latitude. Mission lifespan is designed to last for 7 years. Each Sentinel-2 satellite carries an optical multispectral instrument that provides images in 13 spectral bands with spatial resolutions of either 10, 20, or 60 m (European Space Agency, 2015). ESA delivers Sentinel-2 images either as Level-1C or Level-2A products, which both represent radiometrically and geometrically corrected images, where Level-2A in addition to Level-1C includes atmospheric correction. Products used in our study, are Bottom-of Atmosphere Level-2A products. Bands used are blue (490 nm), green (560 nm), red (665 nm) and NIR (842 nm) bands with a 10 m resolution and the narrow NIR (865 nm) band with a 20 m resolution. With respect to POM measurement dates, corresponding cloud-free satellite images were downloaded and processed. Atmospherically corrected images were downloaded from the official Copernicus Open Access Hub (https://scihub.copernicus.eu/) and processed using the official Sentinel-2 Toolbox (European Space Agency, 2018) software and QGIS software (QGIS Development Team, 2018). Acquisition dates for Sentinel-2 images are given in Table 1 and operating wavelengths are given in Table 2.

Data analysis

Since the narrow NIR band of Sentinel-2 images was only available at a 20 m resolution, all images were resampled using the nearest neighbor method. Thus, the blue, green, red and NIR bands from Sentinel-2 images were down-sampled from 10 m to 20 m resolution.

Due to the higher resolution of POM measurements compared to Sentinel-2 images, i.e. several POM measurements points fell within a single Sentinel-2 image pixel (Figure 4), all POM measurements inside a Sentinel-2 pixel were averaged. By employing this, there was only one corresponding value per POM spectral band for each single image pixel. Hence, 1-to-1 comparison between measurements of the two sensors was achieved. Using different spectral band combinations, various indices were calculated (Table 3).

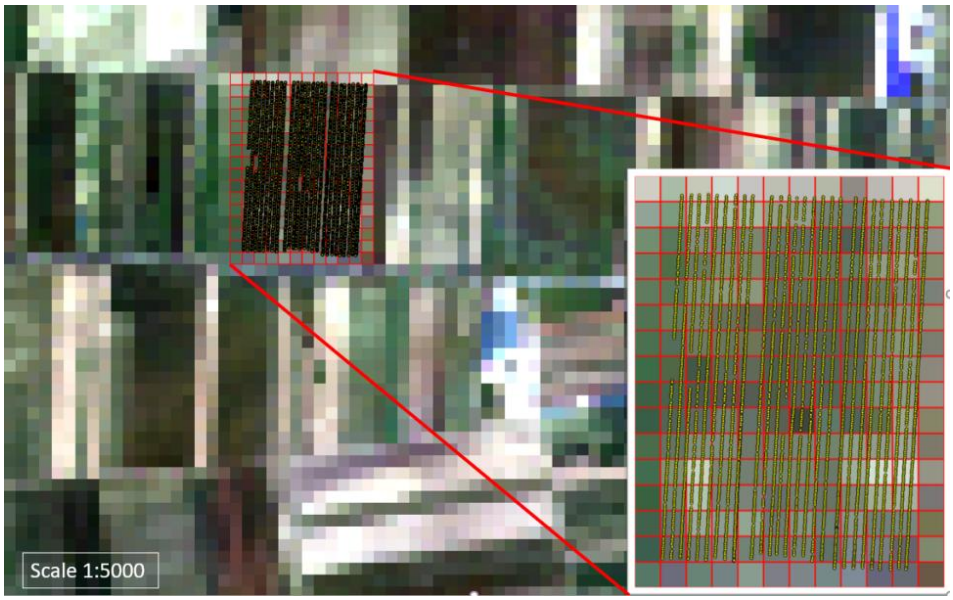

Figure 4. Sentinel-2 image of the experimental field in Begeč at 20 m resolution where yellow dots represent POM measurement points.

Table 3. List of the vegetation indices used in the analysis with given formulas, short description, and further reference.

VI	Formula	Description	Reference
Normalized Difference Vegetation Index	$NDVI = \frac{R_{NIR} - R_{Red}}{R_{NIR} + R_{Red}}$	Most popular vegetation index; indicates plant health status and photosynthetic activity.	(Teal et al., 2006)
Simple ratio	$SR = \frac{R_{NIR}}{R_{red}}$	Indicates greenness of vegetation.	(Rouse et al., 1974)
Infrared Percentage Vegetation Index	$IPVI = \frac{R_{NIR}}{R_{NIR} + R_{red}}$	Functionally equivalent to NDVI, but computationally faster.	(Crippen, 1990)
Green NDVI	$NDVI_g = \frac{R_{NIR} - R_{Green}}{R_{NIR} + R_{Green}}$	More sensitive to chlorophyll concentration variations than NDVI.	(Gitelson et al., 1996)
Blue NDVI	$NDVI_b = \frac{R_{NIR} - R_{Blue}}{R_{NIR} + R_{Blue}}$	Less sensitive to crop stress than NDVI, due to absorption of blue light by anthocyanins and its scattering in the atmosphere.	(Wang et al., 2007, Sentek Systems, 2015)
Structure Insensitive Pigment Index	$SIPI = \frac{R_{NIR} - R_{Blue}}{R_{NIR} - R_{Red}}$	Relates Carotenoids to Chlorophyll a	(Peñuelas and Filella, 1998)

Enhanced Vegetation Index	$EVI = \frac{2.5(R_{NIR} - R_{red})}{R_{NIR} + 6R_{red} - 7.5R_{blue} + 1}$	Sensitive to canopy variations in regions with high biomass, where NDVI saturates.	(Huete et al., 2002)
Green Soil Adjusted Vegetation Index	$GSAVI = 1.5\frac{(R_{NIR} - R_{green})}{R_{NIR} + R_{green} + 0.5}$	Both indices show sensitivity to nitrogen concentration change.	(Sripada, 2005)
Green Optimized Soil Adjusted Vegetation Index	$GOSAVI = \frac{R_{NIR} - R_{green}}{R_{NIR} + R_{green} + 0.16}$		
Green Chlorophyll Index	$GCI = \frac{R_{NIR}}{R_{green}} - 1$	Chlorophyll content estimation	(Gitelson et al., 2003)
Non-Linear Index	$NLI = \frac{NIR^2 - R_{red}}{NIR^2 + R_{red}}$	Minimizes impact of leaf angle distribution, view azimuth and soil brightness	(Goel and Qin, 1994)
Transformed Difference Vegetation Index	$TDVI = 1.5\frac{R_{NIR} - R_{red}}{\sqrt{R_{NIR}^2 + R_{red} + 0.5}}$	Does not saturate like NDVI; minimizes the effect of bare soil beneath vegetation cover	(Bannari et al., 2002)
Wide Dynamic Range Vegetation Index	$WDRVI = \frac{0.2\ R_{NIR} - R_{red}}{0.2\ R_{NIR} + R_{red}}$	Higher sensitivity than NDVI to high values of LAI	(Gitelson, 2004)
Visible Normalized Difference Vegetation Indices	$GRNDVI = \frac{R_{NIR} - (R_{green} + R_{red})}{R_{NIR} + R_{green} + R_{red}}$	VIs constructed with red or blue band are moderately corelated with Leaf Area Index (LAI), whereas those constructed with green band are highly corelated with LAI.	(Wang et al., 2007)
	$GBNDVI = \frac{R_{NIR} - (R_{green} + R_{blue})}{R_{NIR} + R_{green} + R_{blue}}$		
	$RBNDVI = \frac{R_{NIR} - (R_{red} + R_{blue})}{R_{NIR} + R_{red} + R_{blue}}$		
	$PNDVI = \frac{R_{NIR} - (R_{green} + R_{red} + R_{blue})}{R_{NIR} + R_{green} + R_{red} + R_{blue}}$		

Linear regression analysis was elaborated, using the Statistica 13 statistical software (TIBCO Statistica, 2017), to define the relationship between the VIs calculated from the POM measurements and from the Sentinel-2 satellite images. Since Sentinel-2 datasets include two separate bands for the NIR spectrum, the effect of using either one of them in the calculation of the indices was studied. Therefore, the analysis was performed twice: 1) using the wide range NIR band from Sentinel-2 datasets, and 2) using the narrow NIR band.

At the second phase of the data analysis, pixels that were known to be outliers were manually excluded from further analysis. Those were either border pixels, contaminated by the features outside the field, or pixels contaminated by other objects located inside the parcel (Figure 5). Linear

regression analysis was also performed in the outlier-free dataset (after removing the contaminated pixels) to export the final results.

3. RESULTS AND DISCUSSION

The analysis of the Sentinel-2 image acquired on 24 June 2018 provided poor results due to the significant effect of a layer of clouds over the experimental field. Therefore, this date was excluded from the analysis. This is a good example of the constraints of the use of optical satellite images as they highly depend on the weather (Mulla, 2013). Sentinel-2 provides two measurements in the NIR channel: wide (785 – 900 nm) and narrow (855 – 875 nm) range. Therefore, the analysis was performed twice, using the wide range NIR band and narrow NIR band, for the calculation of indices acquired from Sentinel-2 images. In the initial analysis the full dataset regarding the study area, for each of the three useable measurement dates, was used. Regression analysis revealed significant positive correlations between the indices derived from Sentinel-2 satellite images and Plant-O-Meter measurements acquired at V6 growth stage (01-06-2018) before the plants entering the reproductive stages. However, the coefficient of determination (r^2) was considerably low ranging from 0.22 (weakest relationship for EVI) to 0.46 (strongest relationship for $NDVI_{narrow}$, NDVI calculated using narrow NIR band from Sentinel-2, and $PNDVI_{narrow}$, PNDVI calculated using narrow NIR band from Sentinel-2). This was attributed to the existence of contaminated pixels within the dataset that behaved as outliers in the analysis. Those pixels were therefore removed and the regression analysis was repeated with the outlier-free datasets (Figure 5).

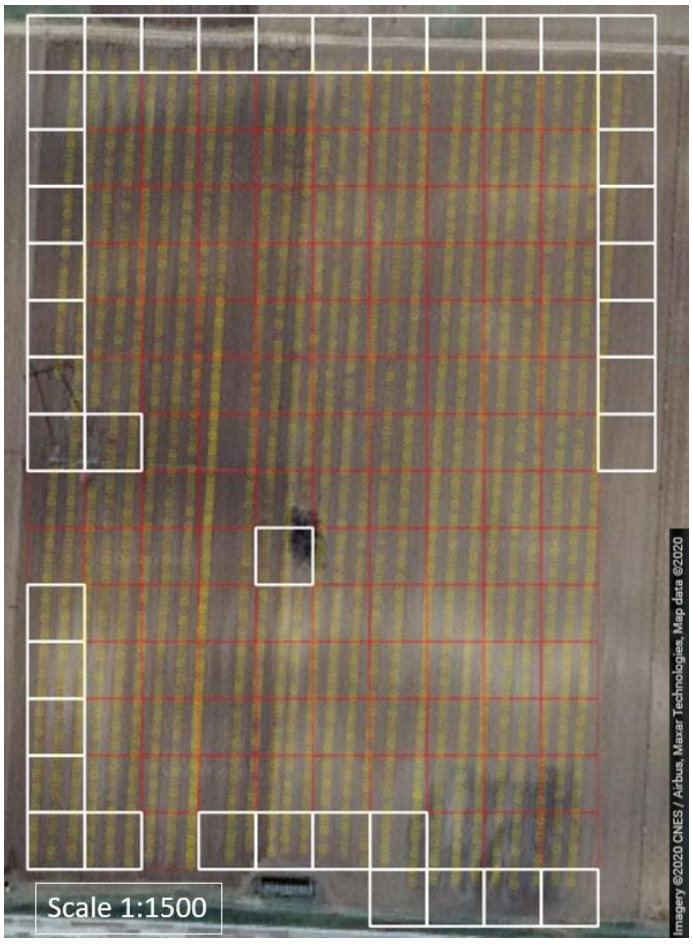

Figure 5. Test field with contaminated pixels (white), pixels used in the analysis (pale red) and POM measurement points (pale yellow); (Google Maps, Imagery ©2020 CNES / Airbus, Maxar Technologies, Map data ©2020).

Table 4. Coefficient of determination (r^2) and Root Mean Square Error (RMSE) from the regression between indices calculated from Sentinel-2, using the wide range NIR band, and POM.

date	01-06-2018		04-07-2018		26-07-2018	
	r^2	RMSE	r^2	RMSE	r^2	RMSE
NDVI	0.680	0.075	0.162	0.093	0.036	0.093
SR	0.612	0.905	0.147	4.283	0.045	4.616
IPVI	0.668	0.045	0.162	0.047	0.036	0.046
NDVIg	0.616	0.058	0.102	0.209	0.008	0.210
NDVIb	0.652	0.103	0.050	0.096	0.000	0.134
SIPI	0.546	0.527	0.059	0.266	0.000	0.267
EVI	0.325	0.182	0.002	0.719	0.000	1.327
GSAVI	0.614	0.091	0.105	0.319	0.008	0.318
GOSAVI	0.615	0.058	0.103	0.210	0.008	0.210
GCI	0.574	0.500	0.087	4.625	0.028	4.611
NLI	0.478	0.014	0.124	0.006	0.060	0.004
TDVI	0.672	0.115	0.167	0.091	0.034	0.089
WDRVI	0.648	0.120	0.156	0.226	0.041	0.230
GRNDVI	0.659	0.062	0.177	0.236	0.022	0.239
GBNDVI	0.676	0.061	0.097	0.244	0.008	0.274
RBNDVI	0.700	0.131	0.143	0.152	0.010	0.184
PNDVI	0.686	0.082	0.155	0.259	0.017	0.288
Average	**0.580**	**0.179**	**0.111**	**0.677**	**0.020**	**0.736**

Table 5. Coefficient of determination (r^2) and Root Mean Square Error (RMSE) from the regression between indices calculated from Sentinel-2, using the narrow range NIR band, and POM.

date	01-06-2018		04-07-2018		26-07-2018	
	r^2	RMSE	r^2	RMSE	r^2	RMSE
NDVI	0.710	0.069	0.162	0.100	0.045	0.103
SR	0.644	0.863	0.135	4.791	0.058	5.615
IPVI	0.696	0.042	0.162	0.050	0.045	0.052
NDVIg	0.630	0.059	0.106	0.217	0.012	0.224
NDVIb	0.676	0.099	0.044	0.101	0.002	0.141
SIPI	0.579	0.522	0.057	0.265	0.001	0.264
EVI	0.344	0.176	0.003	0.715	0.000	1.312
GSAVI	0.627	0.093	0.108	0.331	0.012	0.339
GOSAVI	0.629	0.060	0.107	0.218	0.012	0.225
GCI	0.595	0.515	0.094	5.015	0.032	5.349
NLI	0.493	0.014	0.116	0.006	0.097	0.004
TDVI	0.702	0.106	0.167	0.096	0.043	0.098
WDRVI	0.677	0.114	0.153	0.243	0.052	0.261
GRNDVI	0.683	0.057	0.178	0.248	0.029	0.260
GBNDVI	0.696	0.056	0.095	0.255	0.017	0.293
RBNDVI	0.728	0.124	0.136	0.162	0.022	0.200
PNDVI	0.710	0.076	0.151	0.274	0.028	0.313
Average	**0.603**	**0.175**	**0.110**	**0.733**	**0.028**	**0.842**

The final linear regression analysis provided an insight of which indices calculated using POM are in better agreement with the same ones calculated using Sentinel-2 satellite images. The differences were mainly due to the deviations in the operating wavelengths for the two sensors and in the different sensitivity of each sensor at different bands. According to the statistical analysis, using the narrow range NIR in calculations of Sentinel-2 indices provided better correlation to the POM indices (Table 5; Figure 6b) as compared to the results using the wide range NIR (Table 4; Figure 6a). In the regression between indices calculated from Sentinel-2, using the wide range NIR band (Table 4) for the first date of measurement (V6 growth stage; 01-06-2018), the coefficient of determination (r^2) ranged between 0.325 (for EVI) and 0.700 (for RBNDVI) while the root mean square error (RMSE) ranged from 0.905 (for SR) to 0.014 (for NLI). In the analysis using the Sentinel-2's narrow band NIR,

the coefficient of determination (r^2) was better, ranging between 0.344 (for EVI) and 0.728 (for RBNDVI) while the root mean square error (RMSE) ranged from 0.863 (for SR) to 0.014 (for NLI). This was expected since the measuring range of the narrow NIR band of Sentinel-2 and NIR band of POM, are much closer.

The results for the two measurements during the reproductive stages, silking stage (R1) and blister stage (R2), provided poor results. This is attributed to the fact that after tasselling, the measurements showed considerably lower correlation between the two sensors explained by the mixture of colours after the tassels appear, and the different shades of the canopy from green to yellow as the plants approach maturity. Due to the large difference in the spatial resolution of the measurements of the two sensors in the study, this random mixture of colours affected the results of each sensor differently. The regression results showed low correlation between indices derived by the two sensing systems, showing the coefficient of determination (r^2) lower than 0.178 (Tables 4 and 5). Therefore, these results are not discussed further.

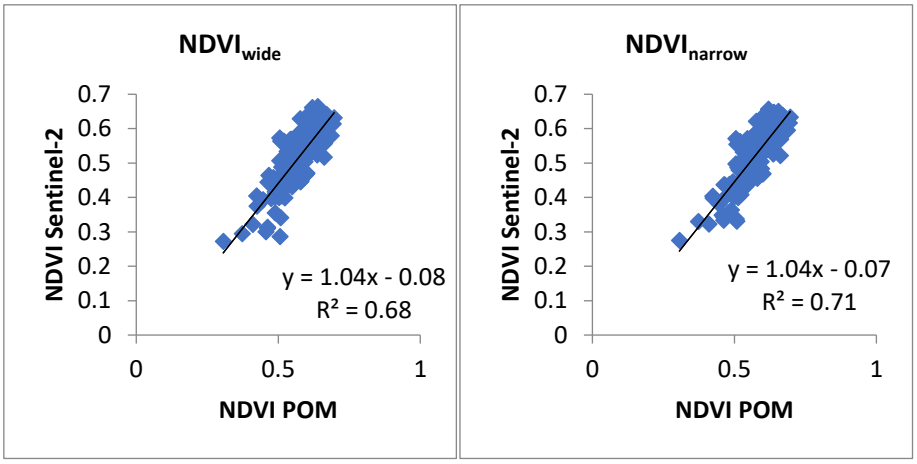

a b

Figure 6. Linear regression between the NDVI calculated from POM measurements and Sentinel-2 satellite images using wide (a) and narrow (b) NIR bands, at V6 maize growth stage.

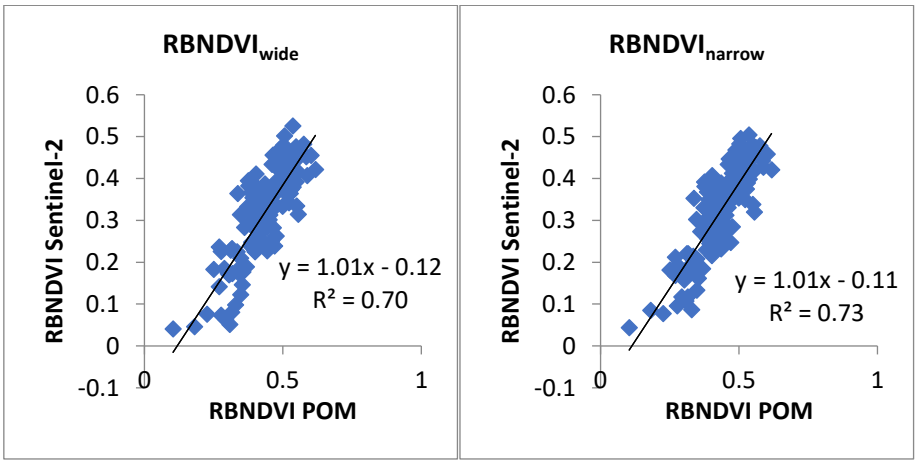

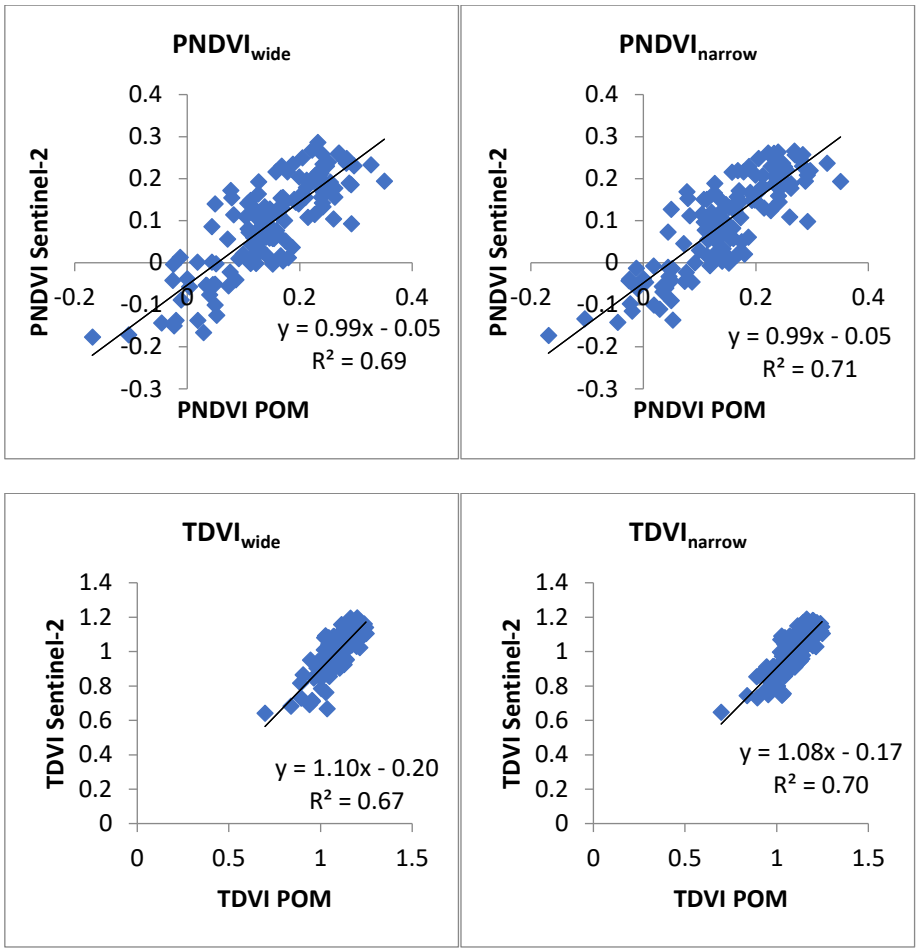

Figure 7. Linear regression between the RBNDVI, TDVI and PNDVI calculated from POM measurements and Sentinel-2 satellite images using wide (left) and narrow (right) NIR bands, at V6 maize growth stage.

The POM measurements acquired at the V6 growth stage showed good correlation with Sentinel-2 results, mainly due to the uniformity of the colour of the area scanned in the field, which at this stage consists crop canopy leaves (green colour). With 6 leaves fully developed, the leaf area covered a significant proportion of the ground without significant overlapping of the vegetation. According to literature, this is the most appropriate stage for remotely sensing the maize crop as this is when the highest spatial variability in the reflectance measurements is observed (Raun et al., 2005).

Concerning the NDVI, which is the most widely used vegetation index (Tagarakis and Ketterings, 2017; Hatfield et al., 2008; Ljubičić et al., 2018), the linear regression showed significant correlation between the POM and Sentinel-2 derived datasets at V6 growth stage for both using the narrow NIR band (r^2= 0.710, RMSE = 0.069; Table 5, Figure 6b) and the wide NIR band (r^2= 0.680, RMSE = 0.075; Table 4, Figure 6a) showing an almost 1:1 relationship; the slope of the linear model approached 1 and the constant approached 0 (Figure 6). The correlation would probably increase if the resolution of the satellite imagery was greater and if the different crop type was scanned which allows minimal reflectance of soil, such as turfgrasses, as reported in (Caturegli et al., 2015). Apart from NDVI, most of the indices showed significant correlations with RBNDVI showing the highest coefficient of determination (r^2 = 0.728) followed by NDVI and PNDVI (r^2= 0.710), and TDVI (r^2= 0.702), (Table 5, Figures 6b and 7 - right). This result suggests that RBNDVI, NDVI, PNDVI, and TDVI calculated using POM are more similar to the Sentinel-2 derived image results and are therefore more preferable to be used in studies that involve both POM (ground-based proximal) and Sentinel-2 (satellite remote) sensors.

The overall results of this study suggest that the POM active proximal multispectral sensor can serve as a good alternative to the Sentinel-2 satellite sensor, having the benefits that the active proximal sensors offer, high spatial resolution, flexibility in the measurement timing and independence from cloudiness (Bu et al., 2017). In addition, satellite data often need auxiliary ground-truth data for correcting the image interpretation (Oerke et al., 2014), and therefore combined use of Sentinel-2 imagery and POM measurements could provide added value in contrast to single source derived information. Attention should be paid to the time of sensing as the measurements acquired by the two different sensing systems (ground-based proximal and satellite-based remote) are dissimilar when the canopy is irregular and the cops' surface shows variability in structure and color, due to the large difference of the spatial resolution.

4. CONCLUSIONS

The present work shows a comparative study among a ground-based proximal multispectral sensor (named Plant-O-Meter) and satellite images from Sentinel-2 mission. Both instruments operate in similar range of specific wavelengths, enabling the calculation of various spectral indices which could be valuable for monitoring crop properties. According to the results, ground-based proximal sensing provides comparable results to the indices calculated from Sentinel-2 satellite images at certain growth stages of maize. Therefore, Plant-O-Meter active proximal sensor can be an alternative to satellite images, providing measurements at high spatial resolution. This system operates independently of weather and illumination conditions overcoming the limitations that passive optical sensors are facing, such as cloudiness, an important limiting factor of satellite remote sensing. Also, since satellite data usually need auxiliary ground-truth data for image interpretation, data fusion of Sentinel-2 imagery and POM measurements may provide added value in contrast to single source derived information.

On the other hand, POM provides information on plant level, while Sentinel-2 is more scalable and can provide information on field or regional level. The plant development stage plays an important role in the agreement between the indices derived by POM and Sentinel-2 due to the large difference in spatial resolution of the measurements. Satisfactory agreement between the indices calculated from the two sensing systems was achieved at progressed growth stages (V6, with 6 fully developed leaves emerged) of maize and before entering the reproductive stages. After the emergence of tassels, the regression between the two datasets provided poor results due to the uneven spatial distribution of the canopy growth and color mixture of leaves and tassels. The results can also apply to other crops; however, additional studies are needed to validate the relationship at the different development stages according to the physiological specifications of each individual crop.

Further use cases may involve the POM proximal crop sensor mounted on tractors or pivot irrigation systems which would, independently or in combination with Sentinel-2 data, enable decision making for variable rate irrigation, fertilization, or fertigation. In addition, the data provided by the two sensing systems will be used for developing and testing algorithms for early- and late-season yield prediction. With an estimated market price below 500 € and a planned commercialization for POM, and in combination with free access to Sentinel-2 data and web applications that utilize satellite data (e.g. AgroSense, 2020), farmers will have an ultimate possibility to apply precision agriculture regardless the size and market share of their business.

ACKNOWLEDGEMENTS

This work was supported by the Ministry of Education, Science and Technological Development of the Republic of Serbia (Grant No. 451-03-68/2020-14/200358), European Union's Horizon 2020 research and innovation programme (Grant No. 739570 – ANTARES) and Provincial Secretariat for

Higher Education and Scientifc Research of Vojvodina through the project “Sensor technologies for integrated monitoring of agricultural production”.

REFERENCES

Adamsen, F.J., Pinter Jr., P.J., Barnes, E.M., LaMorte, R.L., Wall, G.W., Leavitt, S.W. and Kimball, B.A. (1999) ‘Measuring wheat senescence with a digital camera’, Crop Science, 39, pp. 719-724. doi: 10.2135/cropsci1999.0011183X003900030019x.

AgroSense (2020) ‘Digital Agriculture of Serbia’, v3.5.0 https://agrosens.rs/ (accessed January 10, 2020)

Aschbacher, J. and Milagro-Pérez, M. P. (2012) ‘The European Earth monitoring (GMES) programme: Status and perspectives’, Remote Sensing of Environment, 120, pp. 3-8. doi: 10.1016/j.rse.2011.08.028.

Aschbacher, J. (2017) ‘ESA’s Earth Observation Strategy and Copernicus’ In: Onoda, M. and Young, O. R. (eds) ‘Satellite Earth Observations and Their Impact on Society and Policy’, Springer Singapore, pp. 81-86. doi: 10.1007/978-981-10-3713-9.

Atzberger, C. (2013) ‘Advances in Remote Sensing of Agriculture: Context Description, Existing Operational Monitoring Systems and Major Information Needs’, Remote Sens., 5(2), 949-981; doi: 10.3390/rs5020949.

Auernhammer H. (2001) ‘Precision farming — the environmental challenge’, Computers and Electronics in Agriculture, 30, pp .31–43. doi: 10.1016/S0168-1699(00)00153-8.

Bannari, A., Asalhi, H. and Teillet, P. (2002) ‘Transformed Difference Vegetation Index (TDVI) for Vegetation Cover Mapping’, In Proceedings of the Geoscience and Remote Sensing Symposium, IGARSS '02, IEEE International, Volume 5. doi: /10.1109/igarss.2002.1026867.

Bannari, A., Morin, D., Bonn, F. and Huete, A.R. (1995) ‘A review of vegetation indices’, Remote Sensing Reviews 13, 95–120. doi: 10.1080/02757259509532298.

Bausch, W.C. and Khosla, R. (2010) ‘QuickBird satellite versus ground-based multi-spectral data for estimating nitrogen status of irrigated maize’, Precision Agriculture, 11, pp. 274-290. doi: 10.1007/s11119-009-9133-1.

Bu, H., Sharma, L. K., Denton, A. and Franzen, D. W. (2017) ‘Comparison of Satellite Imagery and Ground-Based Active Optical Sensors as Yield Predictors in Sugar Beet, Spring Wheat, Corn, and Sunflower’, Agronomy Journal, 109, pp. 299–308. doi: 10.2134/agronj2016.03.0150.

Campbell, J.B. and Wynne, R.H. (2011) ‘Introduction to Remote Sensing’, Guilford Press, New York, Fifth edition, p. 483. ISBN 978-1-60918-176-5.

Caturegli, L., Casucci, M., Lulli, F., Grossi, N., Gaetani, M., Magni, S., Bonari, E. and Volterrani, M. (2015) ‘GeoEye-1 satellite versus ground-based multispectral data for estimating nitrogen status of turfgrasses’, International Journal of Remote Sensing, 36, pp. 2238–2251. doi: 10.1080/01431161.2015.1035409.

Corti, M., Cavalli, D., Cabassi, G., Gallina, P. M. and Bechini, L. (2018) ‘Does remote and proximal optical sensing successfully estimate maize variables? A review’, European Journal of Agronomy, 99, pp. 37-50. doi: 10.1016/j.eja.2018.06.008.

Crippen R.E. (1990) ‘Calculating the vegetation index faster’, Remote Sens. Environ., 34, pp. 71-73. doi: 10.1016/0034-4257(90)90085-Z.

European Space Agency (2015) 'Sentinel-2 User Handbook', Issue 1, pp. 1-64. https://sentinel.esa.int/documents/247904/685211/sentinel-2_user_handbook (accessed July 25, 2018)

European Space Agency (2018) 'Sentinel Application Platform - SNAP', v6.0.5, http://step.esa.int/main/toolboxes/snap/ (accessed July 25, 2018)

Fitzgerald, G. J. (2010) 'Characterizing vegetation indices derived from active and passive sensors', International Journal of Remote Sensing, 31:16, 4335-4348. doi: 10.1080/01431160903258217.

Fountas, S., Aggelopoulou, K., and Gemtos, T. A. (2016) 'Precision Agriculture', In: 'Supply Chain Management for Sustainable Food Networks', (pp. 41–65), Chichester, UK: John Wiley & Sons, Ltd. doi: 10.1002/9781118937495.ch2.

Gao, B. C. (1996) 'NDWI—A normalized difference water index for remote sensing of vegetation liquid water from space', Remote sensing of environment, 58(3), 257-266. doi: 10.1016/S0034-4257(96)00067-3.

Gavrilov, M.B., Lazić, L., Pešić, A., Milutinović, M., Marković, D., Stanković, A. and Gavrilov, M.M. (2010) 'Influence of hail suppression on the hail trend in Serbia', Phys. Geogr., 31, 5, 441–454. doi: 10.2747/0272-3646.31.5.441.

Gitelson, A.A., (2004) 'Wide Dynamic Range Vegetation Index for Remote Quantification of Biophysical Characteristics of Vegetation', Journal of Plant Physiology 161, 165–173. https://doi.org/10.1078/0176-1617-01176.

Gitelson, A., Gritz, Y. and Merzlyak, M. (2003) 'Relationships Between Leaf Chlorophyll Content and Spectral Reflectance and Algorithms for Non-Destructive Chlorophyll Assessment in Higher Plant Leaves', Journal of Plant Physiology 160, 271-282. doi: 10.1078/0176-1617-00887.

Gitelson, A.A., Kaufman, Y.J. and Merzlyak, M.N. (1996) 'Use of a green channel in the remote sensing of global vegetation from EOS-MODIS', Remote Sens. Environ., 58, pp. 289-298. doi: 10.1016/S0034-4257(96)00072-7.

Goel, N. and Qin, W. (1994) 'Influences of Canopy Architecture on Relationships Between Various Vegetation Indices and LAI and Fpar: A Computer Simulation', Remote Sensing Reviews 10, pp. 309-347. doi: 10.1080/02757259409532252.

Hatfield, J.L., Gitelson, A.A, Schepers, J.S. and Walthall C.L. (2008) 'Application of Spectral Remote Sensing for Agronomic Decisions', Agronomy Journal, 100, pp. 117–131. doi: 10.2134/agronj2006.0370c.

Helman, D., Bonfil, D. J., and Lensky, I. M. (2019) 'Crop RS-Met: A biophysical evapotranspiration and root-zone soil water content model for crops based on proximal sensing and meteorological data', Agricultural Water Management, 211, 210–219. doi: 10.1016/j.agwat.2018.09.043.

Hrnjak, I., Lukić, T., Gavrilov, M.B., Marković, S.B., Unkašević, M., and Tošić, I. (2014) 'Aridity in Vojvodina, Serbia', Theor. Appl. Climatolgy, 115: 323. doi: 10.1007/s00704-013-0893-1.

Huete, A., Didan, K., Miura, T., Rodriguez, E.P., Gao, X. and Ferreira L.G. (2002) 'Overview of the radiometric and biophysical performance of the MODIS vegetation indices', Remote Sensing of Environment, 83, pp. 195-213. doi: 10.1016/S0034-4257(02)00096-2.

Jackson, R. D. (1986) 'Remote Sensing of Biotic and Abiotic Plant Stress', Annual review of Phytopathology, 24, pp. 265-287. doi: 10.1146/annurev.py.24.090186.001405.

Jackson, R.D. and Huete, A.R. (1991) 'Interpreting vegetation indices', J. Preventative Vet. Med., 11, pp. 185-200. doi: 10.1016/S0167-5877(05)80004-2.

Joshi, N., Baumann, M., Ehammer, A., Fensholt, R., Grogan, K., Hostert, P., Jepsen, M.R., Kuemmerle, T., Meyfroidt, P. Mitchard, E.T.A., Reiche, J., Ryan, C. M. and Waske, B. (2016) 'A review of the application of optical and radar remote sensing data fusion to land use mapping and monitoring', Remote Sensing, 8, 70. doi:10.3390/rs8010070.

Khosla, R. (2008) 'The 9th International Conference on Precision Agriculture opening ceremony presentation'. July 20-23rd, 2008.ASA/CSSA/SSSA.

Kitić, G., Tagarakis, A., Cselyuszka, N., Panić, M., Birgermajer, S., Sakulski, D. and Matović, J. (2019) 'A new low-cost portable multispectral optical device for precise plant status assessment', Computers and Electronics in Agriculture 162, 300–308. https://doi.org/10.1016/j.compag.2019.04.021.

Lee, W.S., Alchanatis, V., Yang, C., Hirafuji, M., Moshou, D. and Li, C. (2010) 'Sensing technologies for precision specialty crop production', Computers and Electronics in Agriculture, 74, pp. 2–33. doi: 10.1016/j.compag.2010.08.005.

Liakos, K., Busato, P., Moshou, D., Pearson, S. and Bochtis, D. (2018) 'Machine Learning in Agriculture: A Review', Sensors, 18, 2674. doi: 10.3390/s18082674.

Ljubičić, N., Kostić, M., Marko, O., Panic, M., Brdar, S., Lugonja, P., Knežević, M., Minić, V., Ivošević, B., Jevtic, R. and Crnojević, V. (2018) 'Estimation of aboveground biomass and grain yield of winter wheat using NDVI measurements', Proceedings of the IX International Agricultural Symposium "Agrosym 2018", 390-397. ISBN 978-99976-718-8-2.

McNairn, H., Champagne, C., Shang, J., Holmstrom, D. and Reichert, G., (2009) 'Integration of optical and SyntheticAperture Radar (SAR) imagery for delivering operational annual crop inventories', ISPRS J. Photogramm. Remote Sens., 64 (5), pp. 434-449. doi: 10.1016/j.isprsjprs.2008.07.006.

Mulla, D. J. (2013) 'Twenty five years of remote sensing in precision agriculture: Key advances and remaining knowledge gaps', Biosystems Engineering, Special Issue: Sensing in Agriculture, pp. 358–371. doi: 10.1016/j.biosystemseng.2012.08.009.

Oerke, E.C., Mahlein, A.K., and Steiner, U. (2014) 'Proximal sensing of plant diseases' In: Gullino, M.L., Bonants, P.J.M. (eds) 'Detection and diagnostics of plant pathogens', Springer, Dordrecht, pp 55–68. doi: 10.1007/978-94-017-9020-8_4.

OSRAM Opto Semiconductors (2015) 'Silicon PIN Photodiode Version 1.3.' https://www.osram.com/media/resource/hires/osram-dam-2495839/BPX%2061.pdf (accessed December 17, 2018).

Pandžić, M., Mihajlović, D., Pandžić, J., and Pfeifer, N. (2016) 'Assessment of the geometric quality of Sentinel-2 data', International Archives of the Photogrammetry, Remote Sensing & Spatial Information Sciences, 41, 489–494. doi: 10.5194/isprsarchives-XLI-B1-489-2016.

Pasqualotto, N., D'Urso, G., Bolognesi, S.F., Belfiore, O.R., Van Wittenberghe, S., Delegido, J., Pezzola, A., Winschel, C. and Moreno, J. (2019) 'Retrieval of Evapotranspiration from Sentinel-2: Comparison of Vegetation Indices, Semi-Empirical Models and SNAP Biophysical Processor Approach', Agronomy, 9, 663. doi: 10.3390/agronomy9100663.

Peñuelas, J. and Filella, I. (1998) 'Visible and near-infrared reflectance techniques for diagnosing plant physiological status', Trends Plant Sci, 3, pp. 151-156. doi: 10.1016/S1360-1385(98)01213-8.

QGIS Development Team (2018) 'QGIS Geographic Information System', Open Source Geospatial Foundation Project. http://qgis.osgeo.org (accessed December 28, 2018).

Radičević, Z., Džingalašević, Lj., Bojović, J., Milakara, S. and Radević, S. (2018) 'Agrometeorološki uslovi u proizvodnoj 2017/2018. godini na teritoriji Republike Srbije', Republic

Hydrometeorological Service of Serbia, Division for Applied Climatology and Agrometeorology, QF-E-012, http://www.hidmet.gov.rs/podaci/agro/ciril/AGROveg2018.pdf (accessed January 14, 2020).

Raun, W.R., Solie, J.B., Johnson, G.V., Stone, M.L., Mullen, R.W., Freeman, K.W., Thomason, W.E, and Lukina, E.V. (2002) 'Improving nitrogen use efficiency in cereal grain production with optical sensing and variable rate application', Agron. J. 94:815–820. doi: 10.2134/agronj2002.8150.

Raun, W. R., Solie, J.B., Martin, K.L., Freeman, K.W., Stone, M. L., Johnson, G.V. and Mullen, R.W. (2005) 'Growth stage, development, and spatial variability in corn evaluated using optical sensor readings', J. Plant Nutr., 28, pp. 173-182. doi: 10.1081/PLN-200042277.

Robert, P., Rust, R. and Larson, W. (1994) 'Site-specific Management for Agricultural Systems', Proceedings of the 2nd International Conference on Precision Agriculture, 1994, Madison, WI.

Rouse, J.W., Haas, R.H., Schell, J.A. and Deering, D.W. (1973) 'Monitoring vegetation systems in the great plains with ERTS', Third ERTS Symposium, NASA SP-351, I, pp. 309-317.

Rouse, J.W., Haas, R.H., Schell, J.A., Deering, D.W. and Harlan, J.C. (1974) 'Monitoring the vernal advancement and retrogradation (greenwave effect) of natural vegetation', NASA/GSFC Type III Final Report, p. 371 Greenbelt, Md.

Sentek Systems (2015) 'NDVI DEFINITIONS (RED, BLUE, ENHANCED)' http://www.senteksystems.com/2015/11/23/ndvi-definitions-red-blue-enhanced/ (accessed October 23, 2019)

Shanahan, J.F., Kitchen, N.R., Raun, W.R. and Schepers, J.S. (2008) 'Responsive in-season nitrogen management for cereals', Computers and Electronics in Agriculture, 61, pp. 51-62. doi: 10.1016/j.compag.2007.06.006.

Sripada, R. (2005) 'Determining In-Season Nitrogen Requirements for Corn Using Aerial Color-Infrared Photography', Ph.D. dissertation, North Carolina State University. http://www.lib.ncsu.edu/resolver/1840.16/4200 (accessed January 10, 2020)

Stone, M.L., Solie, J.B., Raun, W.R., Whitney, R.W., Taylor, S.L., and Ringer, J.D., (1996) 'Use of spectral radiance for correcting in-season fertilizer nitrogen deficiencies in winter wheat', Trans. ASAE 39, 1623–1631. doi: 10.13031/2013.27678.

Tagarakis, A. C. and Ketterings, Q. M. (2017) 'In-Season Estimation of Corn Yield Potential Using Proximal Sensing', Agronomy Journal, 109, pp. 1323-1330. doi: 10.2134/agronj2016.12.0732.

Tagarakis A. C. and Ketterings Q. M. (2018) 'Proximal sensor-based algorithm for variable rate nitrogen application in maize in northeast U.S.A.', Computers and Electronics in Agriculture, 145, p. 373-378. doi: 10.1016/j.compag.2017.12.031.

Tagarakis A. C., Ketterings Q. M., Lyons S. and Godwin G. (2017) 'Proximal sensing to estimate yield of brown midrib forage sorghum', Agronomy Journal, 109(1), 107-114. doi: 10.2134/agronj2016.07.0414.

Tagarakis A., Liakos V., Fountas S., Koundouras S. and Gemtos T. (2013) 'Management zones delineation using fuzzy clustering techniques in grapevines', Precision Agriculture 14(1), 18-39. doi: 10.1007/s11119-012-9275-4.

Tattaris, M., Reynolds, M. P. and Chapman, S. C. (2016) 'A direct comparison of remote sensing approaches for high-throughput phenotyping in plant breeding', Front. Plant Sci. 7:1131. doi: 10.3389/fpls.2016.01131.

Teal, R.K., Tubana, B., Girma, K., Freeman, K.W., Arnall, D.B., Walsh, O. and Ruan, W.R. (2006) 'In-season prediction of corn grain yield potential using normalized difference vegetation index', Agron. J., 98, 1488–1494. doi: 10.2134/agronj2006.0103.

TIBCO Statistica (2017) 'Statistica - version 13.3, TIBCO Data Science', TIBCO Software Inc., Palo Alto, CA, USA, www.tibco.com.

Tucker, C. J. (1979) 'Red and photographic infrared linear combinations for monitoring vegetation', Remote sensing of Environment, 8(2), 127-150. doi: 10.1016/0034-4257(79)90013-0.

Wagner, P. and Hank, K. (2013) 'Suitability of aerial and satellite data for calculation of site-specific nitrogen fertilisation compared to ground based sensor data', Precision Agriculture, 14, pp. 135–150. doi: 10.1007/s11119-012-9278-1.

Wang, R., Cherkauer, K. and Bowling, L. (2016) 'Corn Response to Climate Stress Detected with Satellite-Based NDVI Time Series', Remote Sens., 8, 269. doi: 10.3390/rs8040269.

Wang, F., Huang, J., Tang, Y. and Wang, X. (2007) 'New vegetation index and its application in estimating leaf area index of rice', Science, 14 (3), pp. 195-203. doi: 10.1016/S1672-6308(07)60027-4.

Wang, L. and Qu, J. J. (2007) 'NMDI: A normalized multi-band drought index for monitoring soil and vegetation moisture with satellite remote sensing', Geophysical Research Letters, 34(20). doi: org/10.1029/2007GL031021.

Woodcock, C. E., Allen, R., Anderson, M., Belward, A., Bindschadler, R., Cohen, W., Gao, F., Goward, S. N., Helder, D., Helmer, E., Nemani, R., Oreopoulos, L., Schott, J., Thenkabail, P. S., Vermote, E. F., Vogelmann, J., Wulder, M. A. and Wynne, R. (2008) 'Free access to Landsat imagery', Science, 320, pp. 1011. doi: 10.1126/science.320.5879.1011a.

Xue, J. and Su, B. (2017) 'Significant remote sensing vegetation indices: A review of developments and applications', Journal of Sensors, Volume 2017, Article ID 1353691. doi: 10.1155/2017/1353691.

Yang, C., Everitt, J. H., Du, Q., Luo, B. and Chanussot, J. (2013) 'Using High-Resolution Airborne and Satellite Imagery to Assess Crop Growth and Yield Variability'. Proceedings of the IEEE, 101 (3), pp. 582-592. doi: 10.1109/JPROC.2012.2196249.

Yang, C.-M., Liu, C.-C. and Wang, Y.-W. (2008) 'Using Formosat-2 Satellite Data to Estimate Leaf Area Index of Rice Crop', Journal of Photogrammetry and Remote Sensing, 13, pp. 253-260.